Smart Structures and Systems, Vol. 10, No. 6 (2012) 573-591
DOI: http://dx.doi.org/10.12989/sss.2012.10.6.573

Optimal shape of LCVA for vibration control of structures subjected to along wind excitation

Ji-Hun Park[1] and Kyung-Won Min*[2]

[1]*Department of Architectural Engineering, University of Incheon, Incheon, South Korea*
[2]*Department of Architectural Engineering, Dankook University, Yongin, South Korea*

(Received October 28, 2010, Revised September 18, 2012, Accepted October 3, 2012)

Abstract. In this study, a procedure to design an optimal LCVA that maximizes the equivalent damping ratio added to the primary structure subjected to along-wind excitation is proposed. That design procedure does not only consider the natural frequency and damping ratio of the LCVA, but also the proportion of the U-shaped liquid, which is closely related to the participation ratio of the liquid mass in inertial force. In addition, constraints to ensure the U-shape of the liquid are considered in the design process, so that suboptimal solutions that violate the optimal tuning law partly are adopted as a candidate of the optimal LCVA. The proposed design procedure of the LCVA is applied to the control of the 76-story benchmark building, and the optimal proportions of the liquid shape under various design conditions are compared.

Keywords: liquid column vibration absorber; vibration control; equivalent damping ratio

1. Introduction

Various types of vibration absorbers have been developed and applied to real building structures for the vibration control against both wind and earthquakes (Housner *et al*. 1997, Agrawal and Yang 1999, Mazza and Vulcano 2007, Mazza and Vulcano 2011). Recently, many types of the tuned vibration absorber employing liquid as a moving mass are developed, and have been applied to the real tall buildings for the purpose of wind-induced vibration control (Kareem and Kijewski 1999). The liquid-type vibration absorber has many advantages in respect of simple construction and easy maintenance. In the early stage of development, the tuned liquid damper (TLD) that has a simple liquid container in the form of cube or cylinder known as the tuned liquid damper (TLD) was developed and applied (Soong and Dargush 1997). Later, another type of liquid-type vibration absorber adopting a new restoring force mechanism, known as the tuned liquid column damper (TLCD), was developed (Sakai *et al.* 1989). The TLCD utilizes liquid moving in a U-shaped container with a constant cross sectional area, and enables more mass to participate in horizontal inertial force by adjusting horizontal liquid length. Subsequently, the liquid column vibration absorber (LCVA), which is a variation of the TLCD, was proposed by Watkins (1991). The LCVA utilizes a U-shaped container similarly to the TLCD, but its vertical and horizontal liquid columns have different cross sectional area. This feature facilitates design and tuning of the vibration absorber by additional degrees of freedom in design. In addition, many innovative technologies for liquid-type

*Corresponding author, Professor, E-mail: kwmin@dankook.ac.kr

vibration absorbers were developed. TLCD using MR fluid is proposed (Colwell and Basu 2008), and a TMD of which mass is substituted by a TLCD is proposed in order to control bi-directional motion of the primary structure (Heo *et al*. 2009).

Vibration control performance of the tuned mass damper (TMD), which is the most widely-used type of the tuned vibration absorber, depends on three parameters e.g., the mass ratio of the moving mass over the primary structure and the natural frequency and damping ratio of the absorber itself (Soong and Dargush 1997). However, the design of the liquid liquid-type vibration absorber has many differences from that of the TMD in many aspects. Coupled equations of motion for the liquid-type vibration absorber and primary structure differ from those of a typical 2-DOF system applied to the TMD and primary structure. In addition, the moving mass of the LCVA that participates in the inertia-type control force is a fraction of the total liquid mass and is determined by the shape of the container, which is defined by various dimension parameters. As a result, various design results are produced using the same total mass and tuning law, differently from the TMD. In particular, the LCVA has the most degrees of freedom among the liquid-type vibration absorber, and this study focuses on the design of the LCVA.

Hitchock *et al.* proposed and verified an analytical model of the LCVA through free vibration tests of the single-directional and bi-directional LCVAs (Hitchcock *et al.* 1997). Chang and Hsu (1998) proposed an analytical model of the LCVA as well, and analyzed its vibration control performance for various design parameters numerically. Chang and Qu (1998) proposed formulas of the optimal frequency and equivalent damping ratio of the various mass-type vibration absorber including the LCVA, but did not presented how to determine the optimal shape of the LCVA achieving those optimal frequency and damping ratios. Wu *et al.* (2005) proposed design tables of the LCVA, which were calibrated experimentally, through numerical optimization. They showed that the cross sectional area ratio of the LCVA equal to 1.0 is the best for several primary structures. However, they did not take the limit of the liquid displacement into account in their study.

In case of TLCD, which is a special case of the LCVA, many studies were conducted about optimal design. Gao *et al*. (1997, 1999) found the optimal frequency ratio and head loss coefficient with a constraint of the water level displacement below 5% of the liquid length. Yalla *et al.* (2000) proposed optimum absorber parameters of the TLCD for various types of the excitation. Min *et al.* (2005) studied vibration control of the 76-story benchmark building using a single or multiple TLCDs. Shum (2009) proposed closed form optimal solution of the TLCD for suppressing harmonic vibration of the primary structure. However, above studies on the optimal TLCD did not address the relation between the liquid shape and control performance.

In this study, a design procedure of the optimal LCVA that maximizes the equivalent damping ratio added to the primary structure subjected to wind excitation is proposed. That design procedure does not only consider the dynamic characteristics of the LCVA represented by the natural frequency and damping ratio, but also the shape of the liquid which is closely related to the participation ratio of the liquid mass in inertial force. In addition, two constraints on the dimension parameters to achieve the U-shaped liquid and one constraint on the liquid level displacement to maintain the U-shape of the liquid during vibration response are considered to in the design process. The proposed design procedure is verified through a numerical design example for the 76-story benchmark building, and the optimal shapes of the LCVA under various design conditions are compared.

2. Mathematical model

Equations of motion for a MDOF structure coupled with a LCVA are presented as follows (Chang and Qu 1998).

$$M\ddot{X} + C\dot{X} + KX = F - H(G_3\ddot{w} + G_2H^T\ddot{X}) \tag{1}$$

$$G_1\ddot{w} + C_t\dot{w} + K_t w = -G_3H^T\ddot{X} \tag{2}$$

where M, C, K, H are the mass, damping and stiffness matrix of the primary structure and the location matrix of the LCVA, respectively; X and F are the displacement and external force vector of the primary structure, respectively; w is the liquid level displacement; other parameters are given as follows.

$$G_1 = \rho A_V L_e \tag{3}$$

$$G_2 = \rho A_V\,(b/r_A + 2h) = M_t \tag{4}$$

$$G_3 = \rho A_V b \tag{5}$$

$$C_t = 0.5\rho A_V\, r_A \delta|\dot{w}| \tag{6}$$

$$K = 2\rho A_V g \tag{7}$$

where ρ and δ are the liquid density and head loss coefficient of the LCVA, respectively; b and h are dimension of the horizontal length and vertical height of the liquid and represented with other dimension of the liquid container in Fig. 1; r_A is the area ratio between the vertical and horizontal sectional area A_V and A_H, which are calculated from the dimension presented in Fig. 1; L_e is the effective liquid length of the LCVA. In particular, a mass parameter G_2 is equal to the total mass of the liquid. The area ratio and effective liquid length are expressed as

$$r_A = \frac{A_V}{A_H} \tag{8}$$

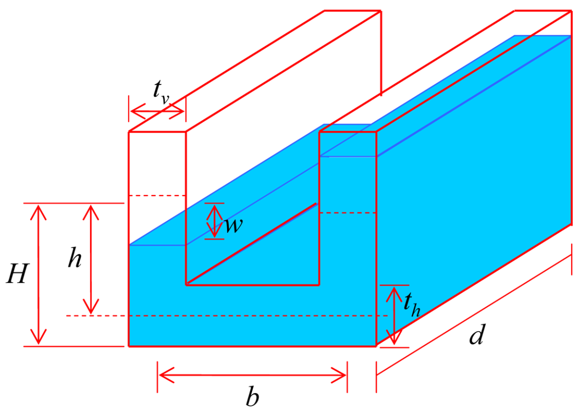

Fig. 1 Dimensions of the LCVA

$$L_e = r_A b + 2h \tag{9}$$

Horizontal liquid motion is r_A times the vertical motion, assuming incompressible liquid. Therefore, G_3 defined by Eq. (5) is a mass parameter to represent inertia force of the horizontal liquid column using the liquid level acceleration $\ddot{w}$ in Eq. (1). Also, G_1 defined by Eq. (3) is a mass parameter to represent inertia forces in Eq. (2), which is related to liquid motion and derived using the Lagrange equation based on energy (Gao *et al*. 1997). K_t defined by Eq. (7) is introduced in Eq. (2) in order to represent restoring forces caused by unbalanced weights between two vertical liquid columns. Equilibrium between inertia and restoring forces in Eq. (2) can be comprehended considering that the liquid pressure at an end of the horizontal liquid column should be the same as the liquid pressure at the bottom of the adjacent vertical liquid column and these two liquid columns have different cross sectional areas.

The equations of motion (1) and (2) are transformed to the following equation retaining only the first mode of the primary structure.

$$\begin{bmatrix} 1+\mu_2 & \mu_3 \\ \mu_3 & \mu_1 \end{bmatrix}\begin{Bmatrix} \ddot{q}_1 \\ \ddot{w} \end{Bmatrix} + \begin{bmatrix} 2\zeta_1\omega_1 & 0 \\ 0 & 2\mu_1\zeta_t\omega_t \end{bmatrix}\begin{Bmatrix} \dot{q}_1 \\ \dot{w} \end{Bmatrix} + \begin{bmatrix} \omega_1^2 & 0 \\ 0 & \mu_1\omega_t^2 \end{bmatrix}\begin{Bmatrix} q_1 \\ w \end{Bmatrix} = \begin{Bmatrix} F_1^*/M_1^* \\ 0 \end{Bmatrix} \tag{10}$$

where q_1, ω_1, ζ_1, M_1^* and F_1^* are the generalized coordinate, natural frequency, damping ratio, generalized mass and external force of the first mode of the primary structure, respectively; ω_t and ζ_t are the natural frequency and damping ratio of the LCVA; μ_1, μ_2 and μ_3 are the mass ratio of the LCVA defined as

$$\mu_1 = \frac{G_1}{M_1^*}; \quad \mu_2 = \frac{G_2}{M_1^*}; \quad \mu_3 = \frac{G_3}{M_1^*} \tag{11}$$

The natural frequency of the LCVA is defined by effective liquid length as follows.

$$\omega_t = \sqrt{\frac{2g}{L_e}} \tag{12}$$

The damping ratio of the LCVA ζ_t is an equivalent linear damping ratio expressed as

$$\zeta_t = \frac{C_t}{2\omega_t} = \frac{\rho A_V r_A \delta \sigma_{\dot{w}}}{\sqrt{2\pi}\,\omega_t G_1} \tag{13}$$

assuming that nonlinearity caused by the response-dependent damping coefficient Eq. (6) is not strong and the liquid level velocity is a stationary Gaussian process (Chang 1998).

3. Wind excitation and response

According to the previous study of Chang and Qu (1998), the external force is modeled with a one-sided power spectral density of the fluctuating component of the wind load, which is defined as

$$S_F = A_1 S_f = A_1 \frac{2s^2}{3\omega(1+s^2)^{4/3}} \tag{14}$$

where ω and A_1 represent the frequency and intensity of the wind excitation, respectively, and s is defined by the following equation.

$$s = \frac{600\omega}{\pi\bar{v}_{10}} \tag{15}$$

where $\bar{v}_{10}$ is the mean wind speed at the height of 10 m.

In Eq. (14), S_F and S_f are one-sided spectrum for the fluctuating wind loading and wind velocity, respectively. In this study, the wind velocity spectrum proposed by Davenport (1971) is adopted for S_f in Eq. (14).

The intensity of the wind excitation A_1 in the Eq. (14) is expressed as

$$A_1 = \frac{\phi_1^T S_P \phi_1}{(M_1^*)^2} \tag{16}$$

where ϕ_1 is the mode vector corresponding to the first mode of the primary structure, and S_P is the cross-correlation coefficient matrix of the wind force acting on each story of the building. S_P is determined by the aerodynamic admittance, which transforms the wind velocities distributed along a building height to the generalized wind force for the first mode and depends on the wind speed profile and drag coefficient of the building (Simiu 1996, Solnes 1997).

RMS responses of the primary structure and LCVA are obtained by the integration of their power spectral densities, as follows.

$$q_{1,RMS}^2 = A_1 \int_0^\infty |H_{q1}(i\omega)|^2 S_f(\omega) d\omega \tag{17}$$

$$q_{1C,RMS}^2 = A_1 \int_0^\infty |H_{q1}^c(i\omega)|^2 S_f(\omega) d\omega \tag{18}$$

$$w_{RMS}^2 = A_1 \int_0^\infty |H_w(i\omega)|^2 S_f(\omega) d\omega \tag{19}$$

$$\dot{w}_{RMS}^2 = A_1 \int_0^\infty \omega^2 |H_w(i\omega)|^2 S_f(\omega) d\omega \tag{20}$$

where $q_{1,RMS}$, $q_{1C,RMS}$, w_{RMS} and $\dot{w}_{RMS}$ denote the RMS of the uncontrolled and controlled generalized coordinate of the primary structure, and the RMS of the liquid level and velocity of the LCVA, respectively, and corresponding transfer functions are denoted by H_{q1}, H_{q1}^c, H_w and $H_{\dot{w}}$, respectively.

Peak responses are obtained by multiplying a peak factor to the corresponding RMS responses. The peak factor is composed of two factors estimating the mean and standard deviation of the peak, respectively, and expressed by the following equations proposed by Davenport (1964).

$$p = \sqrt{2\log \nu t_s} + \frac{0.5772}{\sqrt{2\log \nu t_s}} \tag{21}$$

$$q = \frac{\pi}{\sqrt{6}} \frac{0.5772}{\sqrt{2\log \nu t_s}} \tag{22}$$

where

$$\nu = \omega_1 / \pi \tag{23}$$

and t_s is the duration of the wind excitation assumed as 300 sec. The peak factor p and q estimate the mean and standard deviation of the peak, respectively, and the sum of those two factors is applied to estimate peak responses.

4. Optimal frequency ratio and damping ratio

Generally, a vibration absorber that utilizes a mass-spring system tuned to the primary structure is designed by determining the natural frequency and damping ratio of the absorber for a specific mass ratio. The optimal frequency ratio and damping ratio of the LCVA installed in the primary structure subjected to wind excitation presented by Eq. (10) were proposed by Chang and Qu (1998), and adopted in the procedure to find an optimal liquid shape in this study. The optimal frequency ratio and damping ratio produce an optimal additional equivalent damping ratio expressed by the following equation.

$$\zeta_e = \frac{\gamma\zeta_1\lambda(\zeta_t + \zeta_1\lambda)}{[(1+\mu_2)^2\zeta_t\lambda^4 + \zeta_1 4(1+\mu_2)\zeta_t^2 + \gamma\lambda^3 + \zeta_1 4\zeta^2 + 4(1+\mu_2)\zeta_t^2 + \gamma - 2(1+\mu_2)\lambda^2 + 4\zeta_1\zeta_t^2\lambda + \zeta_t]} \tag{24}$$

where λ and γ are the frequency ratio and the mass-ratio-related parameter respectively, and defined as

$$\lambda = \omega_t / \omega_1 \tag{25}$$

$$\gamma = \mu_3^2 / \mu_1 \tag{26}$$

Chang and Qu proposed the optimal natural frequency ratio λ_{opt} and the optimal damping ratio $\zeta_{t,opt}$, which maximize ζ_e, neglecting the damping ratio of the primary structure. (Hitchcock *et al*. 1997) Those optimal tuning parameters are expressed using only mass ratio μ_2 and mass-ratio-related parameter γ as follows.

$$\lambda_{opt} = \left(\frac{\omega_t}{\omega_1}\right)_{opt} = \frac{(1+\mu_2-\gamma/2)^{0.5}}{1+\mu_2} \tag{27}$$

$$\zeta_{t,opt} = \frac{1}{2}\sqrt{\frac{\gamma(1+\mu_2-\gamma/4)}{(1+\mu_2)(1+\mu_2-\gamma/2)}} \tag{28}$$

Accordingly, the optimal tuning parameters are determined by only three mass ratios μ_1, μ_2 and μ_3. The optimal equivalent damping ratio $\zeta_{t,opt}$ can be converted to the head loss coefficient using Eq. (13).

5. Optimal design of the LCVA shape

There exist various LCVA shapes of which total liquid mass is the same, because the shape of the LCVA is defined by various dimension parameters. Those LCVAs have the same total mass ratio μ_2

but have different combinations of the other two mass ratios μ_1 and μ_3. As a result, they have different optimal frequency ratio λ_{opt} and optimal damping ratio $\zeta_{t,opt}$, which are related to only those three mass ratios, as observed in Eqs. (27) and (28). This means that, even if the same liquid mass is utilized, LCVAs have different vibration control performance relying upon the proportion of their shapes. In this study, the optimal shape and damping parameter of the LCVA, which has a fixed total liquid mass G_2 and maximizes additional equivalent damping ratio for a given range of design parameters, are investigated through parametric study. Several independent design parameters are varied and the other parameters are determined to tune the LCVA according to the optimal frequency ratio and optimal damping ratio given by Eqs. (27) and (28).

5.1 Constraint conditions in the design of the LCVA

Three constraints are imposed in the design of the LCVA. Firstly, the displacement of the liquid level is constrained because the LCVA assumes U-shape of the liquid. If the liquid level becomes lower than the ceiling of the horizontal liquid column, the U-shape is destroyed. This results in the violation of the equation of motion (1) and corresponding failure of optimal tuning. Accordingly, the liquid level displacement should be limited as follows.

$$w_{max} < h - t_h/2 \tag{29}$$

The other two constraints are related to the dimension of the liquid column to ensure the U-shape of the LCVA and expressed as follows.

$$t_v < b \tag{30}$$

$$h > t_h / 2 \tag{31}$$

An optimally designed LCVA considering only the optimal tuning law represented by Eqs. (27) and (28) may violate those three constraints, since those two equations are irrelevant to the above three constraints. In particular, a design result violating constraint Eqs. (30) or (31) is physically infeasible, and should be discarded. However, regarding the first constraint Eq. (29), a suboptimally tuned but feasible solution can be obtained if a damping ratio higher than the optimal one is used to reduce the peak liquid level displacement. In this study, among design solutions satisfying constraint Eq. (29) and optimal tuning frequency Eq. (27), a solution with the optimal damping ratio defined by Eq. (28) is designated as Optimally Tuned Solution (OPTS), while a solution of which damping ratio is higher than the optimal one is designated as Suboptimally Tuned Solution (SOTS). Depending on the combination of the assumed mass ratios and the intensity of the excitation, an OPTS can be obtained without violating the constraints, or a SOTS should be adopted in order to meet the constraints. Even if a SOTS does not satisfy optimal tuning condition, it may have better performance than a OPTS, because the control performance of the LCVA is not only affected by the tuning frequency and damping ratio but also the amount of mass participating in the horizontal inertial force. In addition, the SOTS remains optimal in respect of the frequency ratio, because the optimal frequency ratio defined by Eq. (27) is irrelevant to the damping ratio of the LCVA.

5.2 Design procedures of the LCVA

In the design procedure described bellow, the optimal dimensions and optimal equivalent damping ratio of the LCVA are determined. Overall design procedure of the LCVA is described as follows. In order to obtain a global optimal LCVA for a given mass ratio μ_2 corresponding to the total liquid mass G_2, the other mass ratios μ_1 and μ_3, and the liquid column width d are chosen as independent design variables. An OPTS is obtained for each combination of those design variables within prescribed range. If the OPTS violates the constraint condition on the peak liquid level displacement, the OPTS is substituted with a SOTS. Finally, the additional equivalent damping ratios corresponding to all the feasible optimal solutions are compared to determine the global optimal solution. A procedure to obtain a single feasible solution of the LCVA for a given combination of design variables is summarized as follows.

(Step 1) The liquid column width d, the mass ratio μ_1 and μ_3 are assumed and corresponding liquid mass G_1 and G_3 are calculated.

(Step 2) The optimal frequency and optimal damping ratios corresponding to the three mass ratios are calculated using Eqs. (27) and (28).

(Step 3) The effective liquid length for optimal tuning is calculated based on Eq. (12) as follows.

$$L_e = \frac{2g}{\omega_t^2} \tag{32}$$

(Step 4) The cross sectional area of the vertical liquid column and the horizontal liquid length are calculated using Eqs. (3) and (5).

$$A_V = \frac{G_1}{\rho L_e} \tag{33}$$

$$b = \frac{G_3}{\rho A_V} \tag{34}$$

(Step 5) The cross sectional area ratio r_A is calculated by solving Eqs. (4) and (9) simultaneously.

$$r_A = \frac{s+\sqrt{s^2+4}}{2} \tag{35}$$

where

$$s = \frac{1}{b}\left\{L_e - \frac{G_2}{\rho A_V}\right\} \tag{36}$$

(Step 6) Cross sectional area of the horizontal liquid column and other dimension parameters are calculated.

$$A_H = \frac{A_V}{r_A} \tag{37}$$

$$h = (L_e - r_A b)/2 \tag{38}$$

$$t_V = A_V/d \tag{39}$$

$$t_H = A_H/d \tag{40}$$

(Step 7) Constraints Eqs. (30) and (31) are checked for the designed dimension parameters.

(Step 8) Peak liquid level displacement is calculated using Eq. (19) and the peak factors defined by Eqs. (21) and (22). If constraint Eq. (29) is violated, the equivalent damping ratio ζ_t of the LCVA is increased incrementally, until the peak liquid level displacement is reduced to the threshold.

In Step 8, all dimension parameters are fixed, while ζ_t is increased incrementally. Based on Eq. (13), the final ζ_t can be transformed to the head loss coefficient δ, which can be adjusted by installing orifice in the middle of the liquid column. For the prediction of the head loss coefficient, empirical equations defined by area blocking ratio of the orifice are available (Wu *et al*. 2005), but field vibration tests are recommended for the fine tuning of the head loss coefficient on the final stage of installing a designed LCVA.

6. Design example

6.1 Design condition

In this study, optimal LCVAs are designed for various design conditions considering constraint Eqs. (29) to (30). Design conditions related to the primary structure and wind excitation and LCVA dimensions are summarized in Table 1. The properties of the primary structure are based on the 76-story benchmark building proposed by Yang etc (Yang *et al.* 2004). The total mass of the building is 153,000 ton and corresponding generalized mass of the first mode is 20% of the total building mass. The natural period of the benchmark building is 6.25 sec, and periods of 5.0, 8.0 and 10.0 sec are considered additionally in the design example. The RMS displacement of the primary structure at the location of the LCVA indicates the intensity of the wind excitation. The mass ratio of the total mass of the LCVA over the first modal mass of the primary structure μ_2 is assumed to be 0.01. The intensity of the wind excitation A_1 in Eq. (14) is calculated utilizing Eq. (17) rather than Eq. (16) as follows for convenience.

Table 1 Design condition of the LCVA

Primary structure	Generalized mass (ton)	30,600			
	Damping ratio	0.01			
	Natural period (sec)	5.0	6.25	8.0	10.0
Wind excitation	RMS displacement of the primary structure at the location of LCVA $q_{1,RMS}$ (mm)	100	50 100 150 200	100	100
	Peak factor p	3.28	3.21	3.14	3.06
	Peak factor q	0.24	0.25	0.25	0.26
	Duration t_s (sec)	300 sec			
	Mean wind speed at the height of 10 m $\bar{v}_{10}$ (m/sec)	30 m/sec			
LCVA dimension parameters	d	2.5, 5, 7.5, 10, 12.5, 15, 17.5, 20 m			
	μ_1 (%)	0.04~6.0@0.04			
	μ_2 (%)	1.0			
	μ_3 (%)	0.02~2.0@0.02			

$$A_1 = \frac{q_{1,RMS}^2}{\int_0^{\infty} |H_{q1}(i\omega)|^2 S_f(\omega) d\omega} \tag{41}$$

In the 76-story benchmark building, a vibration control device is assumed to be installed on the top floor and the RMS displacement at this floor without control is assumed to be $q_{1,RMS}$ = 100 mm (Yang *et al.* 2004). In this study, additional RMS displacements at the top floor are considered to investigate the influence of the excitation intensity.

6.2 Optimal design result

The additional equivalent damping ratio ζ_e provided by the LCVA designed for T_1 = 6.25 sec and $q_{1,RMS}$ = 100 mm is represented in Fig. 2, where the damping ratio is represented by the brightness of the surface indicated by the color bar, for different combinations of the mass ratio μ_1 and μ_3. In Fig. 2, it is obvious that there exists an optimal combination of μ_1 and μ_3 that achieves the highest

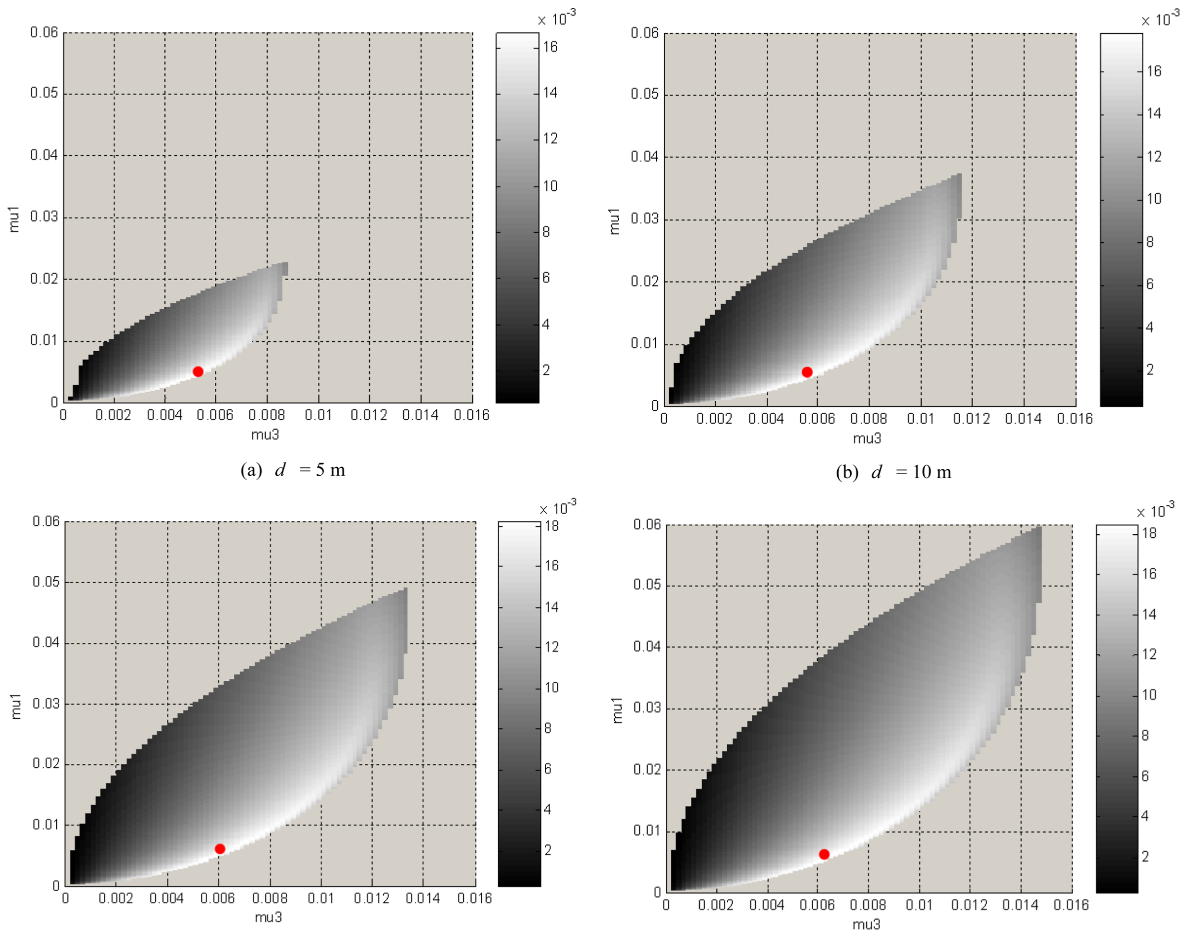

(a) d = 5 m (b) d = 10 m (c) d = 15 m (d) d = 20 m

Fig. 2 Additional equivalent damping ratio (T_1 = 6.25 sec, $q_{1,RMS}$ = 100 mm)

Table 2 Optimal combination of mass ratios (μ_2 = 1%)

T_1 (sec)	$q_{1,RMS}$ (mm)	d (m)							
		5	10	15	20	5	10	15	20
		Mass ratio (%)							
		μ_1				μ_3			
5	100	0.24	0.44	0.52	0.56	0.28	0.44	0.50	0.54
6.25	50	0.24	0.40	0.36	0.50	0.42	0.56	0.54	0.64
6.25	100	0.36	0.44	0.56	0.62	0.46	0.54	0.62	0.66
6.25	150	0.44	0.56	0.66	0.68	0.46	0.56	0.62	0.64
6.25	200	0.52	0.62	0.72	0.76	0.46	0.54	0.60	0.62
8	100	0.46	0.54	0.60	0.70	0.60	0.66	0.70	0.76
10	100	0.50	0.76	0.72	0.68	0.66	0.82	0.80	0.78

additional equivalent damping ratio. Those optimal combination of the mass ratios are marked with a circle for each liquid column width d, and listed in Table 2. Also, it is observed that more combinations of the two mass ratios lead to feasible solutions for larger liquid column width d. This is because reduction of the liquid column width d under the condition of the fixed total liquid mass makes the liquid column thicker and lowers the upper bound of the liquid level displacement.

The movement of the liquid in the horizontal column generates inertia force that controls the vibration of the primary structure. In case of the TMD, the larger the moving mass is, the better the control performance is. Therefore, the mass ratio of the horizontal liquid column to the primary structure is expected to play an important role in the control performance by analogy with the TMD, and is calculated by the following equation and plotted in Fig. 3 for $T_1 = 6.25$ sec and $q_{1,RMS} = 100$ mm.

$$\mu_h = \frac{\rho A_H b}{M_1^*} = \frac{G_3 \cdot r_A}{M_1^*} \tag{42}$$

In Fig. 3, the highest mass ratio of the horizontal liquid column is marked with a circle for each d. Comparing Figs. 2 and 3, the mass ratios μ_1 and μ_3 corresponding to the highest additional equivalent damping ratio are much smaller than those achieving the highest mass ratio of the horizontal liquid column. Those two mass ratios have very low values, because they are proportional to the cross sectional area of the vertical liquid column that should be reduced to obtain larger volume of the horizontal liquid column with the same total liquid mass. Discrepancy between the mass ratios corresponding to the peak points in Fig. 2 and those in Fig. 3 implies that optimal tuning should not be conducted independently after the liquid shape is designed to maximize the horizontal moving mass.

The global optimal values of the additional equivalent damping ratio for different values of the assumed liquid column width d are plotted in Figs. 4(a) and (b). Each global optimal additional equivalent damping ratio is found from their corresponding chart in the form of Fig. 2, and ranges between 0.01 and 0.02. Fig. 4(a) compares the additional equivalent damping ratios for different natural periods of the primary structure. No feasible solutions are found for $T_1 = 5.0$ sec and $d = 2.5$ m. Higher additional equivalent damping ratio is obtained for a primary structure with a longer natural period. By increasing the liquid column width d, higher additional equivalent damping ratios are obtained. In particular, the influence of d is more remarkable for a relatively short-period structure.

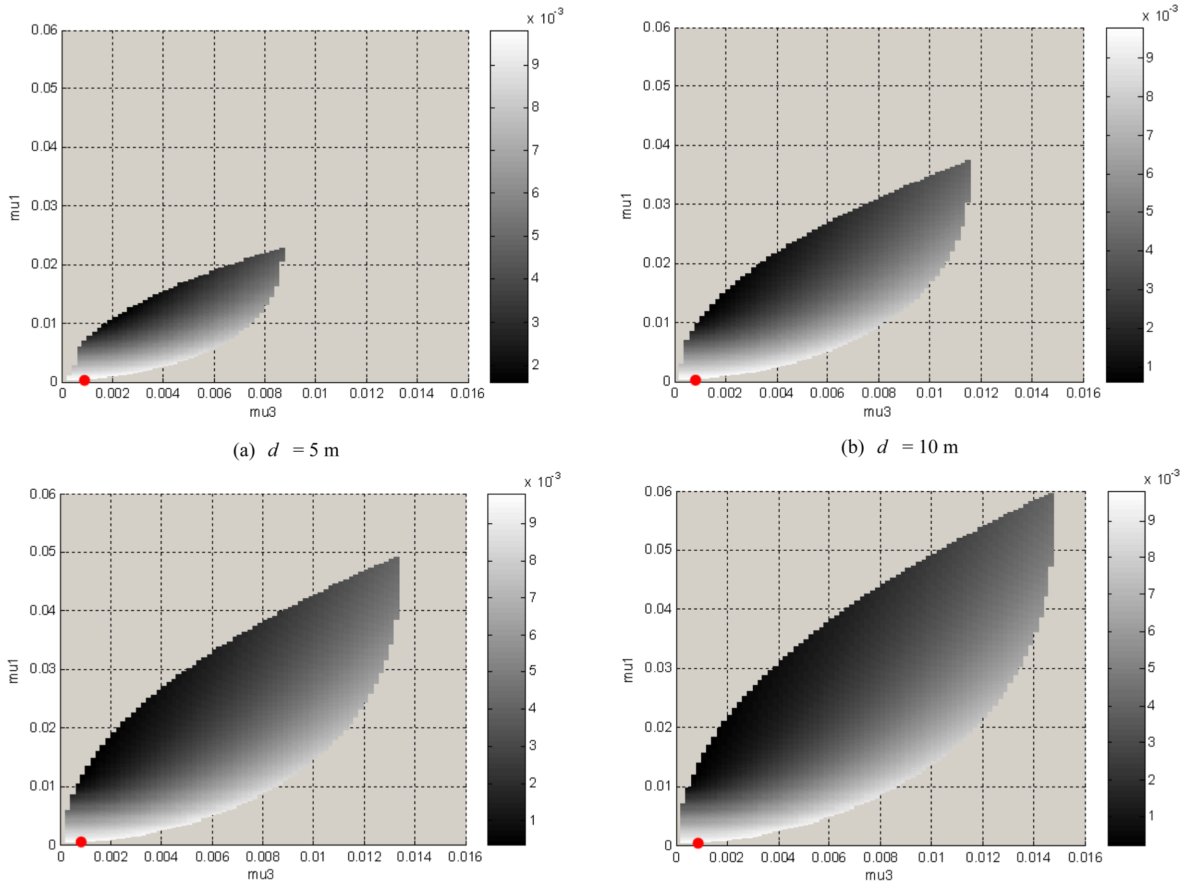

(a) d = 5 m

(b) d = 10 m

(c) d = 15 m

(d) d = 20 m

Fig. 3 Mass ratio of the horizontal liquid column over the primary structure (a,b) (T_1 = 6.25 sec, σ_{q1} = 100 mm), (c,d) (T_1 = 6.25 sec, $q_{1,RMS}$ = 100 mm)

However, since the increasing rate of the damping ratio slows down for higher d, a liquid column width larger than a certain level does not contribute to improving the control performance. Also, the LCVA with a large d may occupy unnecessarily large space of the building floor. The influence of the liquid column width is negligible for the relatively long period of 10 sec. Fig. 4(b) compares the additional equivalent damping ratios for different intensity of the wind excitation for the primary structure of T_1 = 6.25 sec. Larger additional equivalent damping ratios are obtained for smaller intensity of wind excitation, but the improvement by increasing liquid column width is more remarkable for larger intensity of wind excitation.

6.3 Influence of the constraints

In order to check the effects of the constraint on the liquid level displacement, the stochastic peak liquid level displacement of the optimal LCVA of corresponding to each point in Fig. 4 is normalized by its upper limit calculated by Eq. (29), and plotted in Fig. 5. All the normalized liquid level displacements are nearly 1.0 with negligible errors except for the case of T_1 = 10 sec and d =

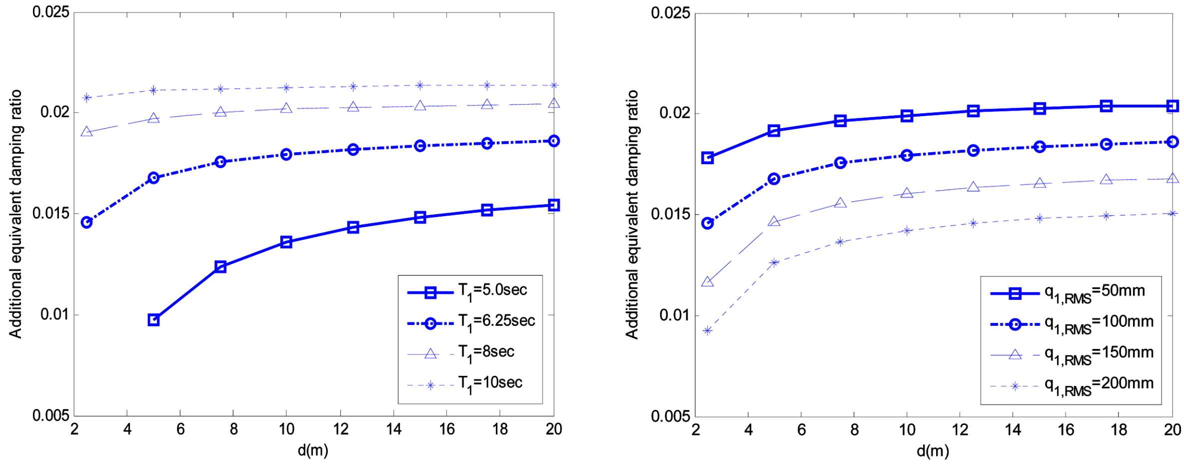

(a) $q_{1,RMS}$ = 100 mm (b) T_1 = 6.25 sec

Fig. 4 Global optimal additional equivalent damping ratio

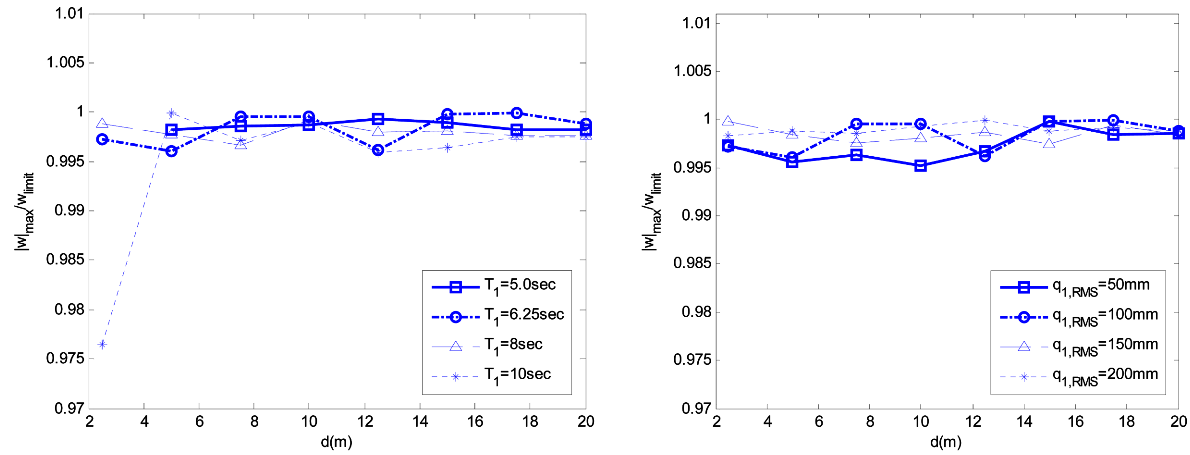

(a) $q_{1,RMS}$ = 100 mm (b) T_1 = 6.25 sec

Fig. 5 Normalized liquid level displacement

2.5 m. This means that the constraint on the liquid level displacement should be considered in the optimal design of the LCVA.

The equivalent linear damping ratios of the SOTS and OPTS corresponding to the global optimal LCVAs for various design conditions are compared in Fig. 6. In the process of searching a global optimal LCVA, an OPTS that does not meet the constraint condition on the liquid level displacement are substituted with a SOTS. The equivalent linear damping ratio of the LCVA corresponding to an OPTS is calculated by the optimal tuning Eq. (28) without considering any constraints. On the other hand, the equivalent damping ratio of the LCVA corresponding to a SOTS is raised to meet the constraint on the liquid level. Discrepancy between those two equivalent damping ratios of the LCVA is larger for the primary structure with shorter natural period in Fig. 6(a), and for stronger wind excitation frequency in Fig. 6(b). A shorter natural period requires shorter equivalent liquid

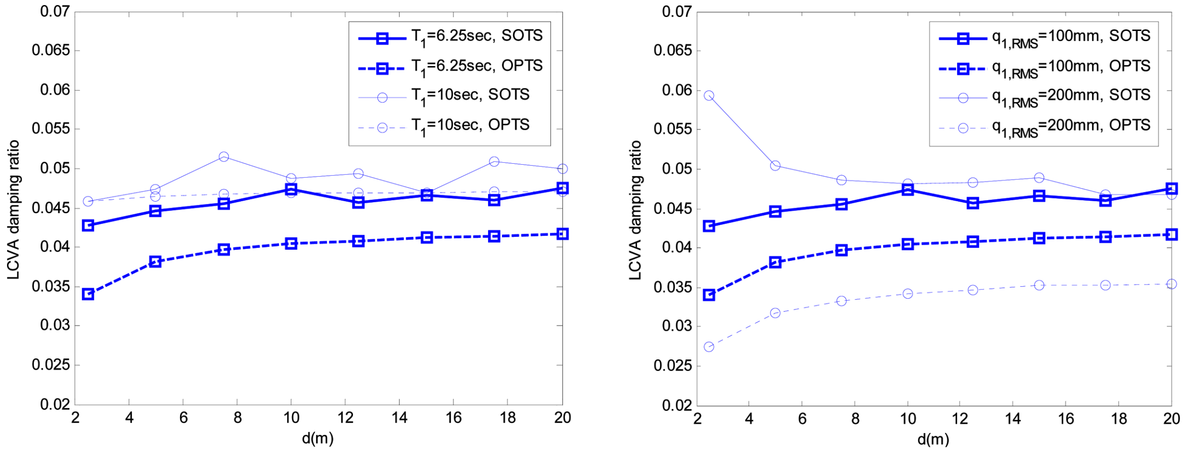

(a) $q_{1,RMS}$ = 100 mm (b) T_1 = 6.25 sec

Fig. 6 Equivalent linear damping ratio of the suboptimally and optimally tuned LCVAs

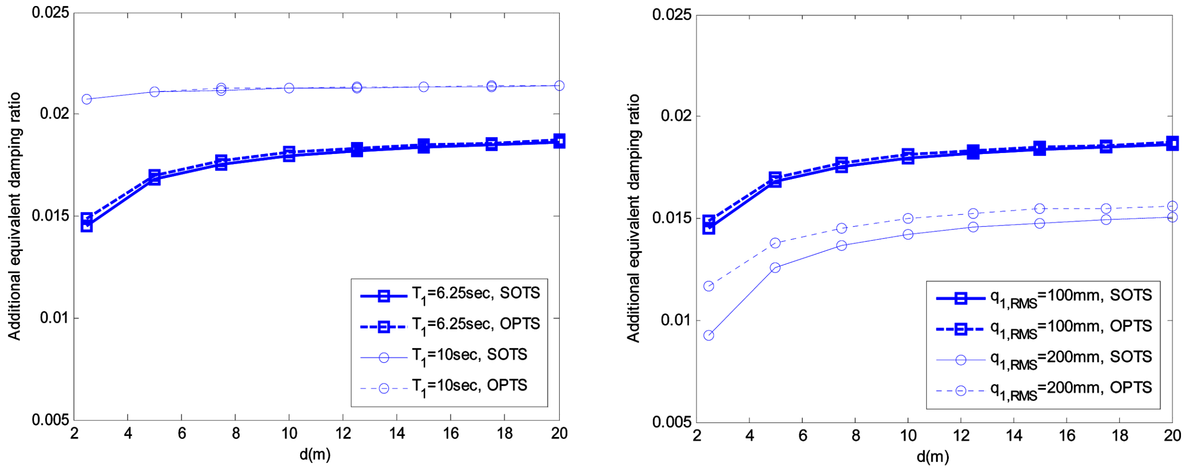

(a) $q_{1,RMS}$ = 100 mm (b) T_1 = 6.25 sec

Fig. 7 Additional equivalent damping ratio achieved by the SOTS and OPTS

length in Eq. (12). Therefore, the vertical liquid column length should be decreased to maintain the volume of the horizontal liquid column that participates in horizontal inertial force. As a result, the equivalent linear damping ratio of the LCVA should be increased to suppress the liquid level displacement below its decreased upper bound. Similarly, stronger wind excitation increases the liquid level displacement so that higher equivalent linear damping is required in the LCVA.

Since the equivalent linear damping ratio of the LCVA in SOTS violates the optimal tuning law, its control performance is expected to be deteriorated. To investigate this loss in control performance, the additional equivalent damping ratios corresponding to SOTS and OPTS are compared in Fig, 7, in which all the design conditions are the same as Fig. 6. The SOTS and OPTS do not have much difference in the additional equivalent damping ratio as shown in Fig. 7 except for the case of $q_{1,RMS}$ = 200 mm, which means relatively strong excitation Therefore, violation of the optimal tuning condition

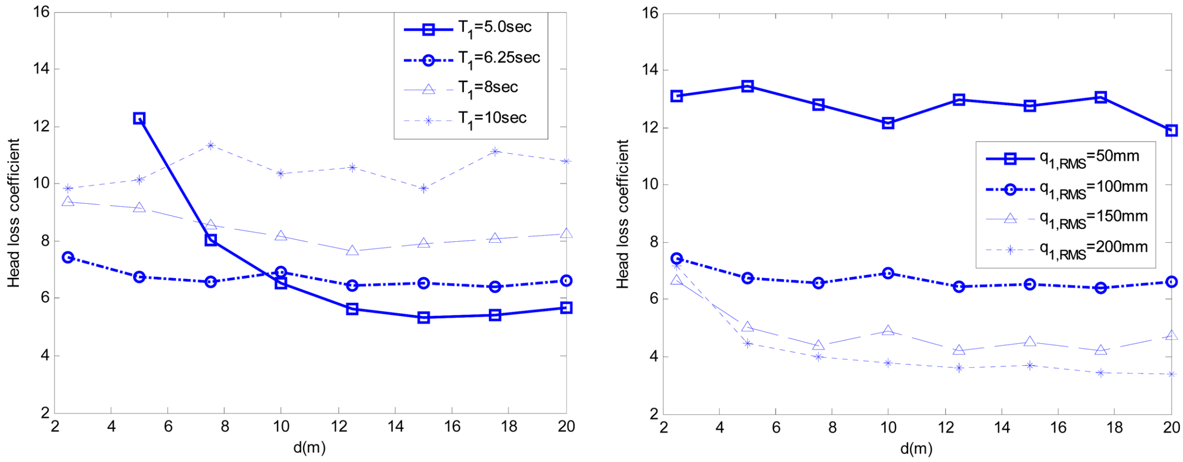

(a) $q_{1,RMS}$ = 100 mm (b) T_1 = 6.25 sec

Fig. 8 Head loss coefficient of the optimal LCVA

in order to obtain a feasible solution affects the control performance a little and can be compensated by increasing the volume of the horizontal liquid column.

6.4 Head loss coefficient

The optimal head loss coefficients corresponding to the equivalent linear damping ratios of the SOTS's are calculated using Eq. (13) and plotted in Fig. 8. It is observed that a longer natural period and weaker wind excitation intensity require a higher head loss coefficient. This is because both conditions cause lower liquid level velocity, to which the head loss coefficient is inversely proportional as shown in Eq. (13) for a given equivalent damping ratio of the LCVA. However, for relatively short natural period (T_1 = 5.0 sec) and strong wind excitation intensity ($q_{1,RMS}$ = 200 mm), optimal LCVAs with small *d*'s need relatively high head loss coefficients. Without this exceptional cases, required head loss coefficient changes little with respect to *d*.

6.5 Optimal shape of the LCVA

Optimal shapes of the LCVA for various natural periods of the primary structure are compared in Fig. 9. The horizontal liquid column length increases, but the vertical liquid column length decreases in Fig. 9, as the natural frequency of the primary structure becomes longer. For the same natural period of the primary structure, the optimal LCVA with a smaller liquid column width has longer and thicker horizontal liquid column in order to distribute more liquid to the horizontal liquid column.

It is noted that a LCVA having a thinner and wider liquid column is more effective since a higher additional equivalent damping ratio is obtained by broader liquid column width as shown in Fig. 4. However, such a LCVA occupies larger area of the building floor and may be impractical design in real construction conditions. Optimal shapes of the LCVA for various wind excitation intensities are compared in Fig. 10. Stronger wind excitation intensity requires shorter horizontal liquid column and longer vertical one due to growing movement of the liquid level.

Cross sectional area ratio r_A of the optimal LCVAs are plotted in Fig. 11. All the r_A's in Fig. 11 are

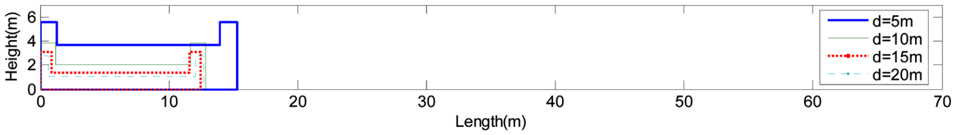

(a) T_1 = 5 sec

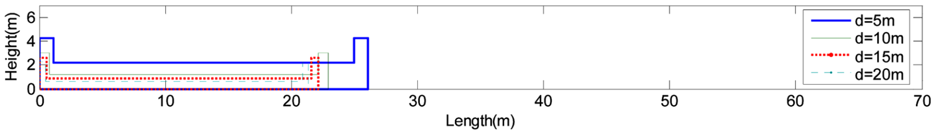

(b) T_1 = 6.25 sec

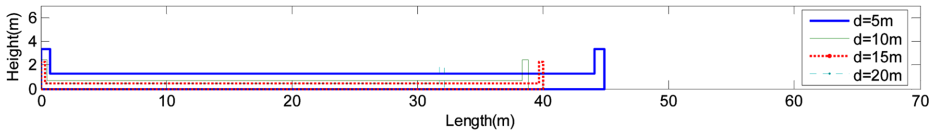

(c) T_1 = 8 sec

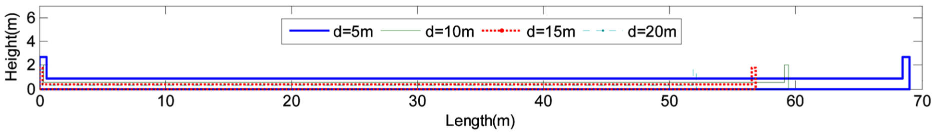

(d) T_1 = 10 sec

Fig. 9 Optimal shape of the LCVA ($q_{1,RMS}$ = 100 mm)

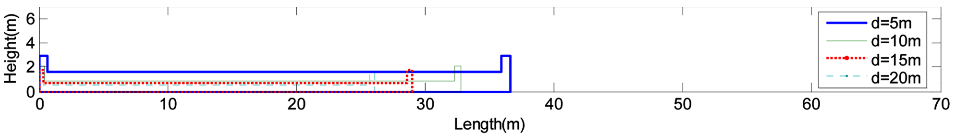

(a) $q_{1,RMS}$ = 50 mm

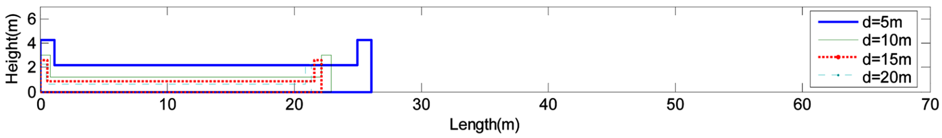

(b) $q_{1,RMS}$ = 100 mm

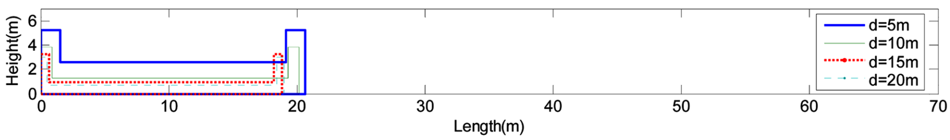

(c) $q_{1,RMS}$ = 150 mm

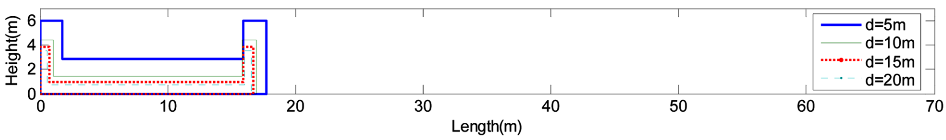

(d) $q_{1,RMS}$ = 200 mm

Fig. 10 Optimal shape of the LCVA (T_1 = 6.25 sec)

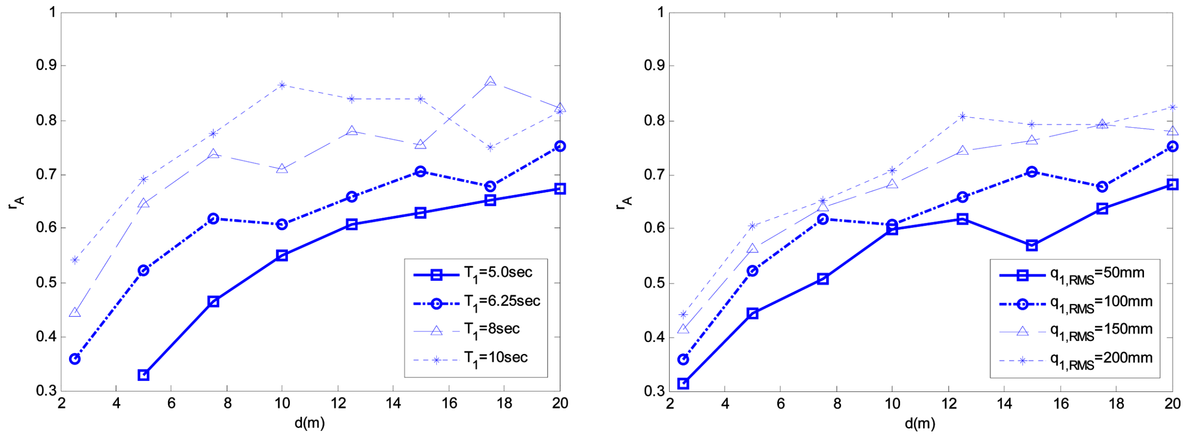

(a) $q_{1,RMS}$ = 100 mm (b) T_1 = 6.25 sec

Fig. 11 Cross sectional area ratio r_A of the optimal LCVA

less than 1.0, which means that horizontal liquid column thicker than vertical one is more efficient in absorbing vibration. For most design conditions presented in Figs. 11(a) and (b), r_A increases as the liquid column width d increases, but the increasing rate of r_A slows down. Besides, r_A shows slightly decreasing tendency for d's higher than 10 m for the two cases of $T_1 = 10.0$ sec in Fig. 11 (a). Wu *et al.* showed that the cross sectional area ratio of the LCVA equal to 1.0 is the best through numerical analysis (Wu *et al.* 2005). The difference between the optimal cross sectional area ratios obtained by this study and Wu *et al.* is caused by constraints on the liquid level displacement, because Wu *et al.* did not take the limit of the liquid displacement into account in their study. Therefore, the constraint of the liquid level displacement and the liquid column width of the LCVA should be considered in the design process to obtain optimal shape of the LCVA.

7. Conclusions

The shape of the LCVA is defined by diverse dimension parameters so that there is an infinite number of LCVAs with the same total mass and natural frequency. In this study, an optimal design procedure of the LCVA focusing on the proportion of the U-shaped liquid is proposed based on the existing optimal tuning law for wind excitation. The proposed design procedure takes constraints on the liquid level displacement and dimension into account to ensure the U-shape of the liquid, and is evaluated thorough numerical design examples. The findings of this study can be summarized as follows.

(1) Besides tuning the frequency and damping ratio, the constraint on the liquid level displacement plays an important role in the optimal design of the LCVA.

(2) The equivalent linear damping ratio of the optimal LCVA is higher than the optimal damping ratio calculated by the unconstrained optimal tuning formula, because the liquid level displacement needs to be suppressed to maintain U-shape of the liquid.

(3) Suboptimal tuning causes little loss of additional equivalent damping ratio to the primary structure.

(4) Larger liquid column width achieves higher additional equivalent damping ratio of the controlled structure, of which increase is more remarkable for short-period structures and strong wind excitation.

(5) The optimal LCVA for a long-period primary structure tends to have long horizontal liquid column, and the optimal one for strong wind excitation has relatively long vertical liquid column.
(6) Smaller liquid column width makes the cross sectional area ratio much smaller than 1.0 so that the horizontal liquid column has much larger volume than that of the vertical one.

Acknowledgements

This work was supported by the Korea Science and Engineering Foundation (KOSEF) grant funded by the Korea government (MEST) (No. R01-2009-00083839) and a grant (Code# '09 R&D A01) from Cutting-edge Urban Development Program funded by Ministry of Land, Transport and Maritime Affairs of Korean Government.

References

Agrawal, A.K. and Yang, J.N. (1999), "Optimal placement of passive dampers on seismic and wind-excited buildings using combinatorial optimization", *J. Intel. Mat. Syst. Str.*, **10**(12), 997-1013.
Chang, C.C. and Hsu, C.T. (1998), "Control performance of liquid column vibration absorbers", *Eng. Struct.*, **20**(7), 580-86.
Chang, C.C. and Qu, W.L. (1998), "Unified dynamic absorber design formulas for wind-indeuced vibration control of tall buildings", *Struct. Des. Tall Spec.*, **7**, 147-66.
Colwell, S. and Basu, B. (2008), "Experimental and theoretical investigations of equivalent viscous damping of structures with TLCD for different fluids", *J. Struct. Eng. - ASCE*, **134**(1), 154-163.
Davenport, A.G. (1961), "The spectrum of horizontal gustiness near the ground in high winds", *Q. J. Roy. Meteorol. Soc.*, **87**(372), 194-211.
Davenport, A.G. (1964), "Note on the distribution of the largest value of a random function with application to gust loading", *Proceedings of the Institution of Civil Engineers*, London.
Gao, H., Kwok, K.C.S. and Samali, B. (1997), "Optimization of tuned liquid column dampers", *Eng. Struct.*, **19**(6), 476-86.
Gao, H., Kwok, K.C.S. and Samali, B. (1999), "Characteristics of multiple tuned liquid column dampers in suppressing structural vibration", *Eng. Struct.*, **21**(4), 316-31.
Heo, J.S., Lee, S.K., Park, E., Lee, S.H., Min, K.W., Kim, H., Jo, J. and Cho, B.H. (2009), "Performance test of a tuned liquid mass damper for reducing bidirectional responses of building structures", *Struct. Des. Tall Spec.*, **18**(7), 789-805.
Hitchcock, P.A., Kwok, K.C.S., Watkins, R.D. and Samali, B. (1997), "Characteristics of liquid column vibration absorbers (LCVA)–I", *Eng. Struct.*, **19**(2), 126-134.
Hitchcock, P.A., Kwok, K.C.S., Watkins, R.D. and Samali, B. (1997), "Characteristics of liquid column vibration absorbers (LCVA)–II", *Eng. Struct.*, **19**(2), 135-44.
Housner, G.W., Bergman, L.A., Caughey, T.K., Chassiakos, A.G., Claus, R.O., Masri, S.F., Skelton, R.E., Soong, T.T., Spencer, B.F. and Yao, T.P. (1997), "Structural control: past, present and future", *J. Eng. Mech. - ASCE*, **123**(9), 897-971.
Kareem, A. and Kijewski, T. (1999), "Mitigation of motions of tall buildings with specific examples of recent applications", *Wind Struct.*, **2**(3), 201-51.
Mazza, F. and Vulcano, A. (2007), "Control of the along-wind response of steel framed buildings by using viscoelastic or friction dampers", *Wind Struct.*, **10**(3), 233-247.
Mazza, F. and Vulcano, A. (2011), "Control of the earthquake and wind dynamic response of steel-framed buildings by using additional braces and/or viscoelastic dampers", *Earth. Eng. Struct. D.*, **40**(2), 155-174.
Min, K.W., Kim, H.S., Lee, S.H., Kim, H. and Ahn, A.K. (2005), "Performance evaluation of tuned liquid column dampers for response control of a 76-story benchmark building", *Eng. Struct.*, **27**(7), 1101-12.

Sakai, F., Takaeda, S. and Tamaki, T. (1989), "Tuned liquid column damper - new type device for suppression of building vibration", *Proceedings of the Conference on High-Rise Building*.

Shum, K.M. (2009), "Closed form optimal solution of a tuned liquid column damper for suppressing harmonic vibration of structures", *Eng. Struct*., **31**(1), 84-92.

Simiu, E. and Scanlan, R.H. (1996), Wind *effects on structures: fundamentals and applications to design*, 3rd Ed., Wiley-Interscience, USA.

Sólnes, J. (1997), *Stochastic processes and random vibrations: theory and practice*, John Wiley & Sons, Chichester, West Sussex, ENG.

Soong, T.T. and Dargush, G.F. (1997), *Passive energy dissipation systems in structural engineering*, Joh Wiley & Sons, USA.

Watkins, R.D. (1991), *Tests on various arrangements of liquid column vibration absorbers*, Research Report R639. School of Civil and Mining Engineering, University of Sydney.

Wu, J.C., Shih, M.H., Lin, Y.Y. and Shen, Y.C. (2005), "Design guidelines for tuned liquid column damper for structures responding to wind", *Eng. Struct*., **27**(13), 1893-1905.

Yalla, S.K. and Kareem, A. (2000), "Optimum absorber parameters for tuned liquid column dampers", *J. Struct. Eng.- ASCE*, **126**(8), 906-15.

Yang, J.N., Agrawal, A.K., Samali, B. and Wu, J.C. (2004), "Benchmark Problem for Response Control of Wind-Excited Tall Buildings", *J. Eng. Mech.- ASCE*, **130**(4), 437-443.

CC